Correlations between Cytotoxicity and Topography of Some 2-Arylidenebenzocycloalkanones Determined by X-ray Crystallography

Jonathan R. Dimmock,*,† Gordon A. Zello,† Eliud O. Oloo,‡ J. Wilson Quail,‡ Heinz-Bernhard Kraatz,‡ Pál Perjési,*,§ Ferenc Aradi,‖ Krisztina Takács-Novák,⊥ Theresa M. Allen,# Cheryl L. Santos,# Jan Balzarini,▽ Erik De Clercq,▽ and James P. Stables○

College of Pharmacy and Nutrition and Department of Chemistry, University of Saskatchewan, Saskatoon, Saskatchewan S7N 5C9, Canada, Department of Medical Chemistry and Central Research Laboratory, University of Pécs, Department of Pharmaceutical Chemistry, Semmelweis University, Budapest, Hungary, Department of Pharmacology, University of Alberta, Edmonton, Alberta T6G 2H7, Canada, Rega Institute for Medical Research, Katholieke Universiteit Leuven, B-3000 Leuven, Belgium, National Institute of Neurological Disorders and Stroke, National Institutes of Health, Bethesda, Maryland 20892-9020

Three series of 2-arylidenebenzocycloalkanones **1**−**3** were prepared in order to compare the topography of the molecules with cytotoxicity. These compounds contain two aryl rings whose spatial relationships to each other were influenced by the size of the alicyclic ring and the nature of the substituents in the arylidene aryl rings. All compounds were evaluated against murine P388 and L1210 cells as well as human Molt 4/C8 and CEM T-lymphocytes. From these results, **1l** and **2c,l** emerged as useful lead molecules and **1l** was shown to significantly inhibit macromolecular DNA, RNA, and protein syntheses in L1210 cells. Various interatomic distances, bond angles, and a torsion angle of 19 representative compounds were determined by X-ray crystallography, and correlations between these data and the cytotoxicity were noted in nearly 40% of the cases examined. Structure−activity relationships revealed that in general, the steric properties of the groups in the arylidene aryl ring, as revealed by measurements of the molar refractivity values, contributed more to bioactivity than the electronic and hydrophobic properties of the aryl substituents. The compounds displayed little murine toxicity, which favors the decision to develop these molecules as cytotoxic and anticancer agents.

Introduction

The principal objective of the present study was to prepare three series of 2-arylidenebenzocycloalkanones **1**−**3** with a view to discern those structural features that influence cytotoxicity (Chart 1).

The design of the compounds in series **1**−**3** was based on the following considerations. First, chalcones or 1,3-diaryl-2-propenones have a variety of bioactivities including cytotoxicity.[1] However, for these molecules, a number of spatial orientations can be adopted and the shapes that elicit bioactivity are therefore difficult to discern. Thus, the restriction of such mobility may be achieved by incorporating the chalcone motif into the 2-arylidenebenzocycloalkanones **1**−**3**. In this way, the location of potentially important groups such as the aryl rings designated A and B (Figure 1), which contribute to cytotoxicity relative to one another, may be identified. The changes in topography in **1**−**3** were anticipated to
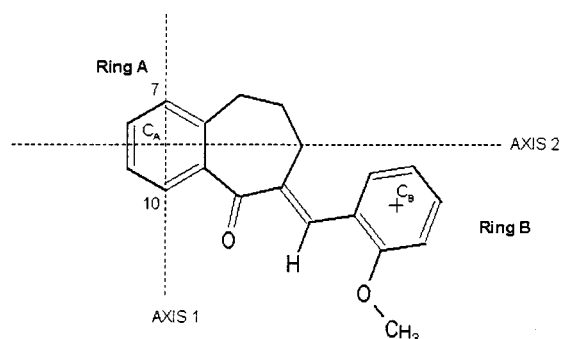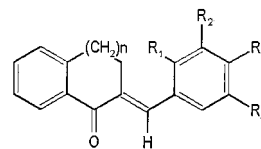

Figure 1. Axes 1 and 2 in relation to a representative compound **3a**.

Chart 1. General Structure of Series 1 (*n* = 0), 2 (*n* = 1), and 3 (*n* = 2).[a]

[a] The nature of the R1−R4 atoms and groups are indicated in Table 1.

be achieved in two ways. In the first place, variation in the size of the cycloaliphatic ring would be expected to alter the relative positions of different functional groups, particularly rings A and B. Second, the introduction of ortho substituents having different sizes into the arylidene aryl ring would be predicted to lead to variation in the torsion angles between the aryl ring

* To whom correspondence should be addressed. J.R.D.: Tel.: 306-966-6331. Fax:306-966-6377. E-mail: dimmock@skyway.usask.ca. P.P.: Tel.: 36(72)536-222. Fax: 36(72)536-225. E-mail: pal.perjesi@oak.pte.hu.
† College of Pharmacy and Nutrition, University of Saskatchewan.
‡ Department of Chemistry, University of Saskatchewan.
§ Department of Medical Chemistry, University of Pécs.
‖ Central Research Laboratory, University of Pécs.
⊥ Department of Pharmaceutical Chemistry, Semmelweis University.
Department of Pharmacology, University of Alberta.
▽ Rega Institute for Medical Research, Katholieke Universiteit Leuven.
○ National Institute of Neurological Disorders and Stroke, National Institutes of Health.

Chart 2. General Structures of Series **4**.[a]
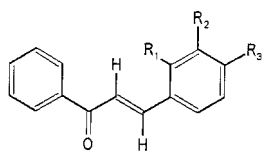
[a] The nature of the R1−R3 groups are indicated in Table 1.

and the adjacent olefinic group. These structural changes may profoundly affect bioactivity.

A second aspect of the design of these molecules was based on a previous observation from these laboratories that 2-(4-methoxyphenylmethylene)benzosuberone possessed 11 times the potency of melphalan when examined against a number of neoplastic cell lines.[2] Hence, the methoxy group was incorporated into different positions of the arylidene aryl ring as displayed in **1a**−**e**, **2a**−**e**, and **3a**−**e**, while different ortho substituents were incorporated into most of the remainder of the molecules.

Furthermore, the evaluation of the compounds outlined in this study for anticonvulsant activity and neurotoxicity in mice was planned for two reasons. First, compounds affording protection against convulsions do so by penetrating the central nervous system (CNS); hence, they may find use in treating CNS tumors. Second, the absence of neurotoxicity and other overt side effects coupled with their cytotoxic activity would enhance the usefulness of these compounds as anticancer agents.

In summary, the decision was made to prepare the compounds **1**−**3**, in which the aryl substitution pattern in ring B was the same in all three series of compounds, and to examine their potential as cytotoxins. Correlations were sought between the topography of representative compounds and the cytotoxicity. A comparison of the cytotoxicity of the 2-arylidenebenzocycloalkanones with the representative acyclic analogues **4a**−**f** (Chart 2) was also proposed.

Chemistry

The compounds in series **1**−**3** were synthesized by the condensation between the appropriate aryl aldehydes and the benzocycloalkanones. Several representative acyclic chalcones **4a**−**f** were also prepared by the same route. [1]H Nuclear magnetic resonance (NMR) spectra were obtained for all compounds. In cases where the olefinic and aryl protons did not overlap, the olefinic protons of the compounds **1**−**3** were detected in the region of 7.2−8.0 ppm indicating the *E* configuration of the chiral axis.[2] The shapes of **1a,d,h,k,l**, **2a,d**−**f,h,j,k**, and **3a,d,e,h**−**j,l** were determined by X-ray crystallography; in all cases, the *E* stereochemistry was noted. The assumption was made, therefore, that all of the compounds **1**−**3** were the *E* isomers. In the case of the chalcones **4**, the coupling constants of the protons on the olefinic group determined by ^{1}H NMR spectroscopy revealed the *E* configuration, an observation that has been noted previously.[3] Molecular modeling was undertaken with **1a,l**, **2a**, and **3a,l**. The redox potentials of three representative compounds **1c**, **2c**, and **3c** were measured. The log *P* figures of **3a**−**l** determined by a reverse phase thin-layer chromatography (TLC) method are summarized in Table 4.

Bioevaluations

All of the compounds in series **1**−**4** were evaluated against murine leukemia P388 and L1210 cells as well as human Molt 4/C8 and CEM T-lymphocytes. These data are presented in Table 1. The inhibitory effects of **1a,l** on the biosynthesis of DNA, RNA, and protein in L1210 cells are summarized in Table 5. Compounds **1**−**4** were examined for anticonvulsant activity and neurotoxicity in mice using doses of either 30 100 or 300 mg/kg.

Discussion

The cytotoxicity evaluation of the compounds **1**−**4** utilized murine P388 and L1210 cells, which are claimed to be good predictors of clinically useful anticancer drugs.[4] In addition, evaluation vs human Molt 4/C8 and CEM T-lymphocytes was undertaken in order to discern whether the compounds would display cytotoxicity toward human tumors. Previous work undertaken with conjugated aryl α,β-unsaturated ketones revealed that the P388 cells were generally more sensitive to enones than other cell lines.[5] Consequently, while a maximum concentration of 50 μM was used in the P388 test, a higher concentration of 500 μM was employed in the L1210, Molt 4/C8, and CEM assays. The data generated are presented in Table 1.

A review of the biodata in Table 1 indicated that in general, the P388 cells were the most sensitive to the enones **1**−**4**. Thus, in those cases where IC_{50} figures were available for all four cell lines, the lowest IC_{50} figures toward P388 cells were noted in 66% of the comparisons made. The average IC_{50} values of **1l**, **2c,l**, and melphalan were 3.61, 3.54, 9.69, and 2.02 μM, respectively, when all four cell lines were taken into consideration, revealing that these three enones are clearly useful lead molecules. The promising activity of **1l** and **2l** may have been due to the molecules per se and/or to reduction of the nitro group to toxic species.[6] A number of cytotoxic compounds possess two aryl rings, which are separated by one or two carbon atoms in which methoxy groups are present on at least one of the aromatic rings. For example, combretastatin A-4 [*Z*-1-(3-hydroxy-4-methoxyphenyl)-2-(3′,4′,5′-trimethoxy)stilbene] interacts at the colchicine site of β-tubulin,[7] and the importance of the presence of a 4-methoxyaryl group for strong interactions has been suggested.[8] It is conceivable, therefore, that the promising activity of **2c** and analogues containing methoxy groups is due, at least in part, to a similar mode of action.

A comparison of the bioactivity between series **1**−**3** was undertaken with a view to determining which spatial orientations of the molecules favored cytotoxicity. The means of the IC_{50} figures of compounds **1**−**3** were compared in order to find if there were differences in the relative potencies between the compounds in series **1**−**3**. One way analysis of variance (ANOVA) tests using equal numbers in groups followed by a series of post-hoc tests, e.g., least significant differences, revealed that the potencies of the compounds in series **1** were significantly lower than the analogues in series **2** and **3** across all screens ($p < 0.1$). In this approach, however, compounds having IC_{50} values of >50 μM in the P388 screen or >20, >100, and >500 μM in the other screens were removed from the analysis along with the ana-

Table 1. Evaluation of the Compounds in Series **1**−**4** against Murine P388 and L1210 Leukemic Cells and Human Molt 4/C8 and CEM T-Lymphocytes[a]

cmpd	R^1	R^2	R^3	R^4	IC_{50} (μM)			
					P388 cells	L1210 cells	Molt 4/C8 cells	CEM cells
1a	OCH_3				28.4 ± 3.5	170 ± 32	308 ± 42	58.2 ± 9.7
1b	OCH_3	OCH_3			28.7 ± 0.7	214 ± 12	53.0 ± 3.3	37.6 ± 7.6
1c	OCH_3		OCH_3		13.0 ± 0.4	14.0 ± 0.7	48.5 ± 37.0	87.1 ± 60.7
1d		OCH_3	OCH_3		23.9 ± 1.8	264 ± 6	468 ± 45	286 ± 120
1e		OCH_3	OCH_3	OCH_3	>50 ± 1.3	>500	>500	>500
1f	CH_3				23.9 ± 1.1	208 ± 94	154 ± 34	56.5 ± 6.1
1g	F				31.7 ± 0.81	150 ± 38	54.2 ± 3.5	47.1 ± 7.6
1h	Cl				26.5 ± 1.63	152 ± 11	128 ± 44	57.0 ± 10.6
1i	Cl		Cl		>50 ± 0.8	>500	>500	>500
1j		Cl	Cl		25.3 ± 1.6	>500	>500	397 ± 146
1k	Br				>50 ± 5.6	64.2 ± 36.8	95.4 ± 4.5	46.8 ± 12.4
1l	NO_2				0.74 ± 0.04	7.61 ± 1.17	2.54 ± 0.61	3.53 ± 2.07
2a	OCH_3				17.5 ± 0.88	40.5 ± 2.9	31.3 ± 1.1	12.6 ± 1.6
2b	OCH_3	OCH_3			12.3 ± 0.6	38.2 ± 2.3	41.3 ± 1.4	28.7 ± 8.7
2c	OCH_3		OCH_3		2.61 ± 0.06	7.98 ± 1.86	1.69 ± 0.20	1.88 ± 0.68
2d		OCH_3	OCH_3		5.69 ± 0.42	42.0 ± 1.3	11.6 ± 0.4	8.55 ± 0.66
2e		OCH_3	OCH_3	OCH_3	6.72 ± 0.6	31.2 ± 0.8	8.28 ± 0.51	7.04 ±0.58
2f	CH_3				17.7 ± 1.0	50.2 ± 7.2	41.4 ± 1.5	43.2 ± 1.8
2g	F				21.8 ± 0.73	22.8 ± 23.5	36.0 ± 2.3	20.8 ± 7.8
2h	Cl				17.5 ± 0.3	30.0 ± 3.7	29.6 ± 5.6	8.80 ± 0.86
2i	Cl		Cl		17.2 ± 0.5	34.4 ± 5.4	28.4 ± 7.6	8.73 ± 1.24
2j		Cl	Cl		13.1 ± 2.3	210 ± 18	28.6 ± 17.0	9.77 ± 0.74
2k	Br				19.7 ± 1.4	33.4 ± 2.0	36.8 ± 1.3	25.4 ± 5.9
2l	NO_2				12.6 ± 1.6	10.8 ± 2.0	8.12 ± 0.44	7.22 ± 1.60
3a	OCH_3				18.0 ± 0.75	46.1 ± 2.5	37.1 ± 1.8	28.9 ± 8.2
3b	OCH_3	OCH_3			8.58 ± 0.7	≥500	≥500	142 ± 64
3c	OCH_3		OCH_3		7.82 ± 0.9	12.4 ± 0.78	71.4 ± 13.8	48.4 ± 13.4
3d		OCH_3	OCH_3		8.19 ± 1.03	≥100[b]	≥20[b]	28.0 ± 10.6
3e		OCH_3	OCH_3	OCH_3	8.68 ± 0.6	35.8 ± 3.8	23.1 ± 8.2	11.7 ± 1.2
3f	CH_3				15.2 ± 0.5	61.2 ± 9.8	36.2 ± 4.9	43.2 ± 1.5
3g	F				13.2 ± 1.6	60.4 ± 26.9	42.1 ± 0.8	28.2 ± 2.4
3h	Cl				12.7 ± 0.93	42.3 ± 4.2	37.1 ± 0.7	18.4 ± 5.0
3i	Cl		Cl		14.0 ± 1.09	≥500	>500	407 ± 131
3j		Cl	Cl		12.2 ± 0.1	45.7 ± 4.5	18.2 ± 1.1	11.8 ± 2.0
3k	Br				19.8 ± 1.5	37.0 ± 2.0	38.4 ± 2.2	32.1 ± 5.6
3l	NO_2				36.5 ± 3.6	47.0 ± 34.2	40.0 ± 15.5	16.2 ± 2.6
4a	OCH_3			−	15.9 ± 1.6	64.4 ± 2.3	8.45 ± 0.37	8.56 ± 0.35
4b		OCH_3		−	9.75 ± 0.7	45.1 ± 4.9	7.94 ± 0.72	8.55 ± 0.04
4c			OCH_3	−	10.63 ±1.3	50.4 ± 7.9	30.0 ± 0.04	33.5 ± 5.5
4d	NO_2			−	3.74 ± 0.2	30.4 ± 7.2	8.38 ± 0.20	8.60 ± 0.30
4e		NO_2		−	15.3 ± 0.5	82.9 ± 41.1	8.53 ± 0.20	8.90 ± 0.80
4f			NO_2	−	7.58 ± 0.8	59.1 ± 61.2	8.32 ± 0.11	13.8 ± 1.6
melphalan[c]					0.22 ± 0.01	2.13 ± 0.03	3.24 ± 0.79	2.47 ± 0.30

[a] For the sake of clarity, only the nonhydrogen substituents in series **1**−**4** are indicated. The dashes indicate the absence of the R^4 group in series **4**. [b] This compound was soluble at 40 μM but insoluble at 200 μM. [c] Reprinted in part from *J. Med. Chem.* **2000**, *43*, 3935. Copyright 2000 American Chemical Society.

logues in the other series having the same aryl substituents. For example, in the P388 screen, **1e,i,k** had IC_{50} figures of >50 μM; hence, **1e,i,k**, **2e,i,k**, and **3e,i,k** were removed from evaluation in these comparisons. In the case of the CEM screen, for example, **1e,i**, **2e,i**, and **3e,i** were not used in the analysis. Therefore, small sample sizes were used in these comparisons.

To include more data, comparisons of the IC_{50} values were made in each series when the aryl substituents were held constant, e.g., the cytotoxicities of **1a**, **2a**, and **3a** in the P388 screen were compared. This approach enabled comparisons to be made when not more than one compound among the three analogues under review did not have a specific IC_{50} value, e.g., >50 μM. The values obtained (Table 1) were ranked with scores of 3, 2, and 1 given to the compounds displaying the highest, intermediate, and lowest potencies, respectively. In assigning scores, the standard deviations of the IC_{50} figures were taken into consideration and the sum of the scores of the relative potencies of each group of three compounds was invariably six. Thus, in the case of **1a**,

2a, and **3a** in the P388 test, scores of 1, 2.5, or 2.5, respectively, were assigned, while in the L1210 screen the figures were 1, 3, or 2, respectively. No comparisons were possible for **1d**, **2d**, and **3d** or between **1i**, **2i**, and **3i** in both the L1210 or the Molt 4/C8 screens due to a lack of specific IC_{50} values for some of the compounds. The total scores for series **1** in the P388, L1210, Molt 4/C8, and CEM screens were 14, 13, 13.5, and 15.5, respectively; for series **2**, the figures were 28.5, 28, 27, and 33.5, respectively; in the case of series **3**, the values were 29.5, 19, 19.5, and 23, respectively. Taking into consideration all four test systems, the average scores for **1**−**3** were 14.0, 29.3, and 22.8. Thus, in three of the four screens, the molecules in series **2** displayed the greater potencies, and in all four tests, series **1** was the least active. Furthermore, the significant differences apparent using ANOVA were confirmed by a nonparametric statistical approach (i.e., Kruskal−Wallis test) using the ranked data, which revealed differences between the three cell lines ($p < 0.001$). One may conclude from the statistical methods that the potencies
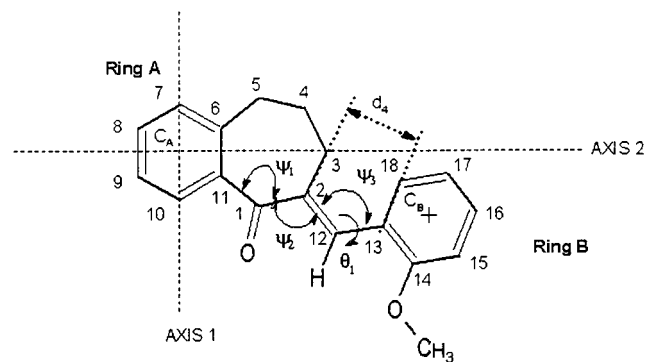
Figure 2. Measurements d_4, $\psi_1-\psi_3$, and θ_1 in a representative compound **3a**.
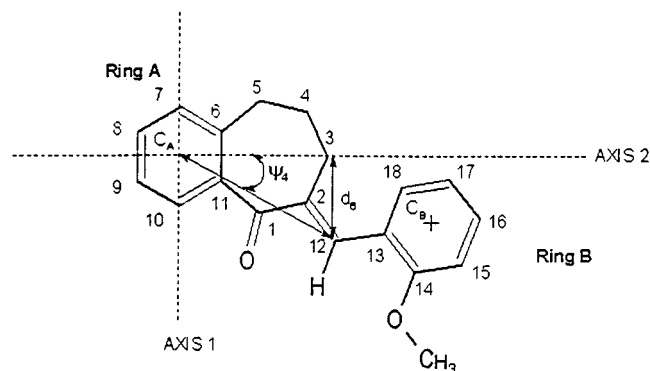

Figure 3. Measurements d_6 and ψ_4 in a representative compound **3a**.

of the compounds in series **2** and **3** were greater than the analogues in series **1**. Overall, the data indicated that cytotoxicity was in the order of **2** > **3** > **1**.

X-ray crystallographic data were obtained on 19 compounds, namely, **1a,d,h,k,l**, **2a,d−f,h,j,k**, and **3a**,**d,e,h−j,l**. The next phase of the study was to determine whether correlations existed between various interatomic distances and bond and torsion angles culled from the X-ray crystallographic data and cyto-toxicity. While the shapes of compounds determined by X-ray crystallography may or may not be identical to the topography of the bioactive species, it is an excellent tool for determining the geometry of molecules. A previous study revealed the importance of the aryl ring attached to the cycloheptanone moiety in eliciting cytotoxicity.[2] Thus, a number of measurements obtained from the X-ray crystallographic data were made in reference to this aryl ring in all three series of com-pounds. In particular, a major emphasis in this inves-tigation was the consideration that cytotoxicity could be correlated with the spatial relationships between the two aryl rings. To investigate this possibility, the centers of aryl rings A and B were designated C_A and C_B, respectively. This procedure is illustrated for a repre-sentative compound **3a** in Figure 1. Axis 1 was con-structed through C7, C_A and C10, and axis 2 was formed at right angles to axis 1 and in the same plane (Figure 1).

The specific measurements made for all of the com-pounds whose structures had been determined by X-ray crystallography were as follows. For the sake of clarity, the nature of some of these determinations is illustrated for **3a** (Figures 2 and 3). Initially, some of the structural characteristics of the linker group between the two aryl
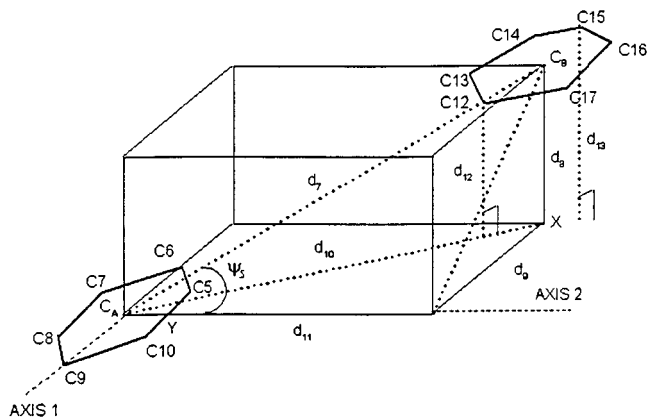

Figure 4. Measurements d_7-d_{13} and ψ_5.

rings were reviewed. The lengths of the C1−C2, C2−C12, and C12−C13 bonds as well as the C2−C13 distances were designated d_1-d_4, respectively (Figure 2). In addition, the distances between the C_A and C12 atoms (d_5) and the C12 atoms and axis 2 (d_6) were recorded (Figure 3). The bond angles $\psi_1-\psi_3$ and torsion angle θ_1 are illustrated in Figure 2, and the angle between the line C_A-C_{12} and axis 2 is referred to as ψ_4 (Figure 3).

To discern the relative positions of the two aryl rings in the benzocycloalkanones, the following data were obtained. Most of these determinations are illustrated in Figure 4. The span between C_A and C_B was desig-nated d_7. The distance of the C_B atoms above or below the plane of ring A is referred to as d_8. In Figure 4, the C_B atom lies above the plane of ring A, as is the case of **3a**, for example. The negative d_8 values indicate those compounds in which C_B is below the plane of ring A. It was obtained by creating a perpendicular from C_B to the plane of ring A at a point X. The perpendicular distance between axis 2 and point X is referred to as d_9. The figures for d_{10} represent the distance between C_A and point X while d_{11} is the span between C_A and the point on axis 2 at right angles to X. To obtain an understanding of the tilt of ring B in relation to ring A, the distances of the C12 and C15 atoms from the plane of ring A were measured and designated d_{12} and d_{13}, respectively. The positive and negative figures pre-sented in Table 2 reflect whether C_{12} and C_{15} were above or below the plane of ring A. Two other portions of these molecules that may influence cytotoxicity were also considered. In the first place, the distance between C_A and the center of the alkylene portion of the cy-cloaliphatic ring d_{14} was recorded (in the case of **3a**, this part of the molecule comprises carbon atoms 3−5 and the attached protons). Second, the distance d_{15} is the span between C_A and the carbonyl oxygen atom.

The X-ray crystallographic data revealed that there was little variation between the d_1-d_4 data. The average d_1-d_4 values were 1.50 (1.49−1.52), 1.34 (1.32−1.36), 1.47 (1.46−1.48), and 2.54 (2.51−2.57) Å, respectively, indicating that these interatomic distances are unlikely to contribute to the differences in cytotoxicity displayed by these compounds. On the other hand, disparate d_5-d_{15}, $\psi_1-\psi_5$, and θ_1 values were noted and these data are presented in Table 2.

To discern whether correlations existed between the cytotoxicity and the interatomic distances d_5-d_{15}, the

Table 2. Interatomic Distances d_5–d_{15} (Å), Bond Angles ψ_1–ψ_5 (deg), and a Torsion Angle θ_1 (deg) of Various Compounds Determined by X-ray Crystallography[a]

compd	d_5	d_6	d_7	d_8	d_9	d_{10}	d_{11}	d_{12}	d_{13}	d_{14}	d_{15}	ψ_1	ψ_2	ψ_3	ψ_4	ψ_5	θ_1
1a	4.80	0.24	7.23	−0.18	1.53	7.23	7.07	−0.12	−0.25	2.52	3.76	106.5	118.7	132.0	2.9	12.3	−178.7
1d	4.81	0.20	7.17	−0.23	1.68	7.16	6.96	−0.14	−0.34	2.51	3.76	106.8	119.9	130.4	2.4	13.7	178.8
1h	4.79	0.19	7.19	0.07	1.69	7.19	6.98	0.01	0.12	2.52	3.77	107.6	119.3	131.2	2.3	13.6	177.5
1k	4.80	0.21	7.19	0.05	1.71	7.18	6.98	0.08	0.03	2.50	3.76	106.0	118.5	130.0	2.5	13.8	−176.9
1l	4.80	0.23	7.18	0.21	1.67	7.18	6.98	0.05	0.38	2.52	3.76	106.4	119.0	129.7	2.7	13.6	174.6
2a	5.06	1.42	7.66	−0.18	0.64	7.66	7.63	−0.16	−0.19	2.84	3.65	117.9	116.2	129.9	16.3	5.0	−149.0
2d	5.09	1.44	7.69	−0.48	0.73	7.68	7.64	−0.31	−0.64	2.84	3.65	117.9	116.4	130.3	16.4	6.5	147.4
2e	5.07	1.38	7.62	−0.51	0.59	7.61	7.58	−0.30	−0.73	2.83	3.64	118.6	117.9	130.1	15.8	5.9	147.3
2f	5.08	1.29	7.55	0.28	0.20	7.55	7.55	0.07	0.48	2.83	3.65	117.7	118.9	127.0	14.7	2.6	−135.6
2h	5.08	1.32	7.57	−0.41	0.23	7.56	7.56	−0.21	−0.59	2.83	3.65	117.5	118.4	127.1	15.0	3.5	137.6
2j	5.10	1.50	7.65	−1.34	0.71	7.54	7.50	−0.87	−1.78	2.84	3.66	117.7	117.1	128.5	17.1	11.4	152.4
2k	5.08	1.42	7.67	0.09	0.62	7.67	7.65	0.23	−0.04	2.84	3.64	118.0	116.6	128.7	16.3	4.7	147.7
3a	5.11	1.75	7.67	1.83	1.21	7.45	7.35	1.22	2.42	2.94	3.61	119.0	117.3	128.3	20.0	16.6	138.2
3d	5.13	1.75	7.75	1.48	1.41	7.61	7.47	0.98	2.00	2.97	3.61	119.2	116.8	130.0	20.0	15.3	150.2
3e	5.07	1.47	7.71	0.56	1.02	7.69	7.62	0.31	0.83	2.98	3.60	119.7	116.4	132.4	16.9	8.7	164.0
3h	5.13	1.99	7.72	1.91	1.65	7.48	7.29	1.30	2.51	2.97	3.61	119.5	116.5	127.5	22.8	19.1	132.4
3i	5.14	2.07	7.72	2.07	1.62	7.43	7.25	1.47	2.63	2.97	3.62	119.2	116.6	127.0	23.8	19.9	132.4
3j	5.08	1.49	7.72	−0.67	1.04	7.69	7.62	−0.36	−0.99	2.98	3.61	119.1	116.9	131.6	17.0	9.2	−166.7
3l	5.12	1.78	7.67	2.05	1.10	7.39	7.30	−1.40	2.70	2.93	3.69	118.5	116.6	126.9	20.4	17.7	139.3

[a] The positive and negative interatomic distance figures indicate that the locations of one of the atoms is above or below the plane of aryl ring A, respectively. The positive and negative θ_1 values signify that the torsion angle is clockwise and anticlockwise, respectively.

Table 3. Correlations Noted between Various Interatomic Distances and Bond Angles Obtained by X-ray Crystallography and Cytotoxicity

distance or bond angle	screens[a]	distance or bond angle	screens[a]
d_5	L1210[b] (−0.464) Molt 4/C8[c] (−0.631)	d_{14}	L1210[c] (−0.498) Molt 4/C8[c] (−0.623)
d_6	L1210[b] (−0.473) Molt 4/C8[c] (−0.622)	d_{15}	P388[b] (0.404) L1210[c] (0.514)
d_7	L1210[c] (−0.482) Molt 4/C8[c] (−0.640)		Molt 4/C8[c] (0.610)
d_9	Molt 4/C8[b] (0.481) CEM[b] (0.412)	ψ_1	L1210[c] (−0.488) Molt 4/C8[c] (−0.642)
d_{10}	P388[b] (−0.405) L1210[c] (−0.488) Molt 4/C8[c] (−0.613)	ψ_2	L1210[c] (0.479) Molt 4/C8[c] (0.607)
		ψ_4	L1210[b] (−0.473) Molt 4/C8[c] (−0.621)
d_{11}	L1210[b] (−0.469) Molt 4/C8[c] (−0.603)	ψ_5	CEM[b] (0.418)

[a] Pearson's r value is in parentheses. [b] $p < 0.1$. [c] $p < 0.05$.

angles ψ_1–ψ_5, and the torsion angle θ_1, which had been determined by X-ray crystallography, bivariate correlation analysis was undertaken. In this process, linear plots of the IC_{50} values of the compounds determined in each cell line were made against the individual distances and angles. Semilogarithmic plots were also determined but did not lead to any changes in the statistically significant correlations obtained using the linear plots. Hence, only the latter are presented in Table 3. Correlations were noted in 37% of the cases. These data revealed that of the 17 physicochemical measurements, i.e., d_5–d_{15}, ψ_1–ψ_5, and θ_1, 12 of these determinations exerted statistically significant effects on cytotoxicity in at least one cell line. The extent of influence upon bioactivity was dependent on the screen under consideration since the percentage of correlations noted in the P388, L1210, Molt 4/C8, or CEM screens was 8, 40, 44, or 8, respectively.

The correlations were negative, except for the d_9 and d_{15} distances as well as the ψ_2 and ψ_5 angles. Thus, elevation of potencies was achieved by decreasing the distances between the following groups, namely, (i) ring A and the olefinic carbon atom (d_5), (ii) the olefinic carbon atom and axis 2 (d_6), (iii) the aryl rings (d_7, d_{10},

and d_{11}), and (iv) ring A and the alkylene portion of the molecules (d_{14}). In addition, potency was increased as the magnitude of the ψ_1 and ψ_4 angles was reduced. On the other hand, lengthening both the distances between ring B and axis 2 (d_9) and the span between ring A and the carbonyl oxygen atom (d_{15}) led to increased cytotoxicity. Bioactivity was increased as the ψ_2 and ψ_5 angles rose. These correlations established the important observation that the spatial orientations of the aryl rings in the 2-arylidene-1-benzocycloalkanones contributed to bioactivity on a number of occasions. Of particular note was the observation that the d_{10} and d_{15} distances correlated with cytotoxicity in three of the four screens. Thus, in the future, the preparation and bioevaluation of different series of compounds that take into consideration these correlations may lead to analogues with greater cytotoxicity.

A second physicochemical method was employed in order to confirm the variation in topography displayed by the compounds in series **1**–**3**. Molecular modeling was undertaken with **1a,l**, **2a**, and **3a,l**, and the d_1–d_{15}, ψ_1–ψ_5, and θ_1 values were obtained. The percentage differences between the X-ray crystallographic and molecular modeling data were less than 6.1% in the case of the d_1–d_5, d_7, d_{10}, d_{11}, d_{14}, d_{15}, and ψ_1–ψ_3 determinations; in fact, these differences were less than 3% in the majority of the comparisons made. The d_6 and ψ_4 data, determined by X-ray crystallography and molecular modeling, revealed that the percentage differences for **1a,l** were 31 and 52; in contrast, the figures for **2a**, and **3a,l** were less than 6%. However, differences of up to 97% were noted in virtually all of the comparisons when d_8, d_9, d_{12}, d_{13}, ψ_5, and θ_1 determinations were considered.

Linear and semilogarithmic plots were undertaken between the d_1–d_{15}, ψ_1–ψ_5, and θ_1 values of **1a,l**, **2a**, and **3a,l**, generated by molecular modeling, and the IC_{50} figures in each of the four cytotoxicity screens. Correlations were noted between the d_2 and ψ_2 figures and potency in the P388 screen and the d_2–d_4 and ψ_3 values in the L1210, Molt 4/C8, and CEM assays. Thus, correlations were noted in five of the 17 measurements

Table 4. Log P Values of **3a–l**

compd	log P^a	compd	log P^a
3a	4.69 ± 0.09	**3g**	4.55 ± 0.06
3b	4.54 ± 0.06	**3h**	5.04 ± 0.04
3c	5.01 ± 0.08	**3i**	5.65 ± 0.01
3d	4.13 ± 0.07	**3j**	5.71 ± 0.05
3e	4.29 ± 0.05	**3k**	5.04 ± 0.02
3f	4.92 ± 0.11	**3l**	4.07 ± 0.07

^{a} The data for **3a,f–h,k,l** are taken from *J. Planar Chromatogr.* **2001**, *14*, 42. Reproduction with permission of the copyright owner.

and in 21% of the evaluations made. These relationships were all positive except for the ψ_2 data. This evidence suggests that the bioactivity observed is correlated with various interatomic distances and bond angles to a greater extent using the data generated by X-ray crystallography rather than molecular modeling.

Linear and semilogarithmic plots were made between specific IC$_{50}$ values of the compounds in each of the series **1–3**, where available, and the electronic (Hammett σ and/or Taft σ^* values), hydrophobic (π constants), and steric [molar refractivity (MR) figures] properties of the aryl substituents. The following correlations were noted. The σ and/or σ^* constants of the compounds in series **3** influenced cytotoxicity significantly in the Molt 4/C8 screen, while the π values of the aryl substituents in series **2** correlated with the IC$_{50}$ figures in the L1210 screen. The MR constants of the series **2** compounds were correlated with cytotoxicity in the P388 and Molt 4/C8 screens, while in series **3** these constants correlated with the cytotoxic properties in the P388 and L1210 series. Negative correlations were noted in all cases except for the π/L1210 relationship in series **2**. One may conclude that in general, steric factors in series **2** and **3**, as determined using MR values that are related to London dispersion forces, influenced cytotoxicity more than the electronic and hydrophobic properties of the molecules. Hence, insertion of small groups into the arylidene aryl ring should be borne in mind when considering the development of this cluster of compounds.

The log P values of the compounds in series **3** were determined, and the results are portrayed in Table 4. Linear and semilogarithmic plots between these figures and the π values of the aryl substituents in **3a–l** revealed an excellent correlation ($p < 0.001$). However, no correlations were noted when, in a similar fashion, the log P figures were plotted against the IC$_{50}$ data generated in each of the four screens (>20, >100, and >500 μM figures were ignored). These data confirm that the relative hydrophobicities of the molecules in series **3** were not correlated with cytotoxicity.

The acyclic analogues of **1a**, **2a**, and **3a** and **1l**, **2l**, and **3l** were prepared; namely, **4a,d**, respectively. These compounds were evaluated for cytotoxicity, and the results are presented in Table 1. The chalcone **4a** had lower IC$_{50}$ figures than the rigid analogues **1a**, **2a**, and **3a**, when three of the four cell lines were examined. However, in general, the IC$_{50}$ values of **1l** and **2l** were lower than that of **4d**; hence, one cannot deduce whether cytotoxicity is enhanced by the relative rigidity or flexibility of these molecules. In general, the placement of the methoxy and nitro substituents in the ortho position of the aryl ring favored cytotoxicity in contrast to the meta and para locations.

Table 5. Effect of **1a,l** on DNA, RNA, and Protein Biosyntheses in L1210 Cells^a

	IC$_{50}$ (μM)			
compd	DNA synthesis	RNA synthesis	protein synthesis	L1210 proliferation
1a	407	292	167	170
1l	14.7 (27.7)	11.7 (25.0)	17.2 (9.71)	7.61 (22.3)
melphalan^b	>100	>100	94.6	2.13

^{a} The figures in parentheses indicate the fold increase in potency of **1l** as compared to **1a**. ^{b} Reprinted in part from *J. Med. Chem.* **2001**, *44*, 586. Copyright 2001 American Chemical Society.

Correlations have been noted previously between the redox potentials of α,β-unsaturated ketones and the cytotoxicity.[1] In the present investigation, in each series, compounds with comparatively high cytotoxicity (**1c**, **2c**, and **3c**) were chosen as well as analogues possessing significantly lower bioactivity (**1i**, **2i**, and **3i**). The E_p values of **1c**, **2c**, and **3c** were 1571, 1560, and 1513 mV, respectively, while no peak potentials were obtained for **1i**, **2i**, and **3i**. The combined Taft σ^* and Hammett σ values for the 2,4-dimethoxy and 2,4-dichloro substituents were −0.50 and 0.61, respectively. Thus, while cytotoxicity is undoubtedly influenced by many considerations, a contributing factor is the extent to which a compound receives or donates electrons in the cells. This observation suggests that the incorporation of strongly electron-donating substituents into aryl ring B may lead to compounds with significant cytotoxicity.

To gain more insight into the possible mechanisms of action of these compounds, two representative enones with markedly different cytotoxicities were chosen. The ortho nitro indanone **1l** was 22 times more potent than the methoxy analogue **1a** in the L1210 screen (Table 1). The data in Table 5 reveal that this disparity in bioactivities is positively correlated with the inhibition of the biosyntheses of DNA, RNA, and protein. While **1l** possessed approximately one-third of the potency of melphalan, its mode of action with regard to the effects on macromolecular biosyntheses is different from the established cytotoxic alkylating agent. Therefore, these compounds may find use against melphalan-resistant tumor cells, an observation that has been made for the Mannich bases of certain α,β-unsaturated ketones.[9]

To address the question of whether the α,β-unsaturated ketones described in this study either penetrated the CNS, displayed neurotoxicity, or were lethal to mice using doses up to and including 300 mg/kg, the following experiments were conducted. The compounds **1a–l**, **2a–l**, **3a–l**, and **4a–f** were administered intraperitonally to mice and were examined in the maximal electroshock (MES) and subcutaneous pentylenetetrazole (scPTZ) screens, which are claimed to be predictors of antiepileptic drugs.[10] In addition, the neurotoxicity of these compounds was determined.[11] Specific details are summarized in the Experimental Section. The enones **2f** and **4a,d** afforded protection in the MES test, and anticonvulsant activity was demonstrated in less than half of the animals in the scPTZ screen by **2j**, **3e**, and **4a**. One-third of the compounds displayed neurotoxicity; however, in general, these results were noted using the higher doses of 100 and 300 mg/kg and observed in less than half of the animals. No mortalities were noted in the neurotoxicity screen. To examine whether CNS activity or neurotoxicity would be demonstrated when

the compounds were administered orally, representative compounds that were active (**2f** and **4a**) or inactive (**1h,i** and **2i**) in the mouse intraperitoneal MES screen were administered orally to rats and activity (or lack thereof) in the MES and neurotoxicity screens was observed at various time intervals. Using a dose of 30 mg/kg, protection against seizures in 25% of the animals was demonstrated in the case of **1h**, **2f**, and **4a**, while none of the five compounds demonstrated neurotoxicity. One may conclude that it is likely that both CNS penetration and neurotoxicity are minimal in these compounds and the absence of deaths at the highest dose of 300 mg/kg enhances their potential as candidate anticancer drugs.

Conclusions

The cytotoxic evaluation of three series of 2-arylidenebenzocycloalkanones revealed that the presence of a six- and seven-membered alicyclic ring favored bioactivity. From the biodata generated, **1l**, and **2c,l** emerged as lead molecules, a viewpoint strengthened by the lack of marked murine toxicity in this group of compounds. The future development of these compounds should bear in mind the correlations between cytotoxicity and those physicochemical parameters established by X-ray crystallography and other structure−activity relationships.

Experimental Section

Melting points were determined on a Boetius apparatus at a heating rate of 4 °C/min and are uncorrected. Elemental analyses (C, H) were undertaken at the Department of Organic Chemistry, Eötvös Loránd University, Budapest, Hungary, on unreported compounds **1c,k**, **2c,i,k**, and **3b,d,e,h** as well as those compounds whose melting points differed from literature values, namely, **1j**, **2b,e**, **3c**, and **4d,e** and were within 0.3% of the calculated figures. Column chromatography was undertaken using kieselgel (Reanal, Hungary) and an eluting solvent of toluene. The purity of compounds was evaluated by TLC using Merck silica gel 60 F_{254} aluminum sheets and developing solvents of either toluene or toluene:ethanol (4:1). ^{1}H NMR spectroscopy was recorded using Perkin-Elmer R12A (60 MHz) or JEOL FX90Q (90 MHz) instruments on all compounds in deuteriochloroform (0.4 M solutions, except for saturated solutions used in the case of **1i,j**). Tetramethylsilane was used as the internal standard. IR spectra were determined using a Nicolet Impact 400 FTIR spectrometer on all compounds as potassium bromide disks, while 0.2 M chloroform solutions of **3a−l** were also recorded.

Syntheses of Compounds. The compounds in series **1−4** were prepared by a base-catalyzed condensation between the appropriate ketone and the aryl aldehyde using a literature method,[12] except for **1g,l**, **2g,l**, and **3l**, which were prepared under acidic conditions.[13] The compounds were purified by column chromatography and subsequently by recrystallization from methanol expect for **2f,g** and **3f,g**, which were recrystallized from hexane. The melting points (°C) of unreported compounds were as follows: **1c**, 126−128; **1k**, 137−139; **2c**, 125−127; **2i**, 108−110; **2k**, 78−80; **3b**, 105−107; **3d**, 146−148; **3e**, 137−139; and **3h**, 76−78. The melting points of several compounds that were different from reported values and those obtained in the present study were as follows: **1j**, 206−208; **2b**, 79−81; **2e**, 109−111; **3c**, 122−124; **4d**, 118−120; and **4e**, 141−143. The remaining compounds had melting points in accord with literature values. The ^{1}H NMR spectra of representative compounds were as follows: **1f**: 2.48 (s, 3H, CH_3), 3.80−4.00 (m, 2H, CH_2), 6.95−8.10 (m, 9H, aryl and olefinic H); **2f**: 2.37 (s, 3H, CH_3), 2.98 (m, 4H, CH_2CH_2), 6.95−8.35 (m, 8H, aryl H), 7.97 (quasi s, 1H, olefinic H); **3f**: 1.60−3.10 (m, 6H, $CH_2CH_2CH_2$), 2.34 (s, 3H, CH_3), 7.05−7.95 (m. 8H, aryl H), 7.97 (quasi s, 1H, olefinic H); **4a**: 3.90 (s, 3H, OCH_3),

6.80−8.35 (m, 11H, aryl and olefinic H). The infrared spectra of **1f**, **2f**, **3f**, and **4a** determined in chloroform revealed carbonyl frequencies of 1696, 1663, 1664, and 1661 cm^{-1}, respectively.

X-ray Crystallography of 1a,d,h,k,l, 2a,d−f,h,j,k, and 3a,d,e,h−j,l. Suitable crystals were obtained from the compounds produced by our syntheses, with the exception of **1a**, which was crystallized from hexane−dimethyl sulfoxide by vapor diffusion at 4 °C. An ω scan was used for data collection. The structures of **1a,h,k,l**, **2a,d**, and **3a,d,l** were solved by XTAL 3.4[14] while NRCVAX[15] was used to determine the structures of **1d**, **2e,j**, and **3e,h**. The SHELX-97 program[16] was used to solve the structures of **2f,h,k**, and **3i,j**. Refinement was undertaken using SHELX-97. Atomic scattering factors were taken from the literature.[17] All nonhydrogen atoms were found on the E-map and were refined anisotropically. Hydrogen atom positions were calculated and not refined. The figures were generated by ORTEP[18] as implemented in Xtal 3.4.

The distances d_1−d_3, bond angles ψ_1−ψ_3, and torsion angle θ_1 were obtained directly from the X-ray crystallographic data. X-ray crystallographic coordinates were loaded into a Macro-Model 4.5 program[19] in order to facilitate the determination of the distances d_4−d_7, d_{14}, and d_{15} and angles ψ_4 and ψ_5. The distances d_8, d_{12}, and d_{13} were obtained using the LSQPL program in XTAL 3.4. The d_9−d_{11} figures were calculated as follows. The distance d_9 was obtained from the relationship $d_9 = (d_{10}^2 - d_{11}^2)^{1/2}$, while for d_{10} the figure was calculated from the equation $d_{10} = (d_7^2 - d_8^2)^{1/2}$. The distance d_{11} was derived from the relationship $d_{11} = d_7\cos\psi_5$.

Molecular Modeling of 1a,l, 2a, and 3a,l. Models of **1a,l**, **2a**, and **3a,l** were built using the MacroModel 4.5 program,[19] which was followed by a Monte Carlo search for the lowest energy conformations using an amber force field on 2000 initial conformations of each compound. Interatomic distances and angles were obtained from the lowest energy conformations by direct measurements or standard geometrical procedures. Evaluation of the relationships between the d_1−d_{15}, ψ_1−ψ_5, and θ_1 figures and cytotoxicity revealed the following correlations [screen, linear (l), or semilogarithmic (sl) plots, p value, Pearson's r value]. d_2: P388, l, <0.1, 0.810; P388, sl, <0.05, 0.981; L1210, sl, <0.1, 0.849; Molt 4/C8, sl, <0.1, 0.836; CEM, sl, <0.1, 0.825. d_3: L1210, sl, <0.05, 0.966; Molt 4/C8, sl, <0.05, 0.933; CEM, l, <0.05, 0.903. d_4: L1210, l, <0.05, 0.966; L1210, sl, <0.1, 0.794; Molt 4/C8, l, <0.05, 0.969; Molt 4/C8, sl, <0.1, 0.805; CEM, l, <0.05, 0.981; CEM, sl, <0.1, 0.814. ψ_2: P388, sl, <0.1, −0.826. ψ_3: L1210, l, <0.05, 0.983; L1210, sl, <0.1, 0.832; Molt 4/C8, l, <0.05, 0.980; Molt 4/C8, sl, <0.1, 0.842; CEM, l, <0.05, 0.986; CEM, sl, <0.1, 0.835.

Statistical Analyses Using σ/σ^*, π, and MR Values. The Hammett σ values were taken from the literature,[20] and the Taft σ^* figures were from a reference source.[21] The Hansch π values were obtained from published data.[22] The MR figures, which were taken from the literature,[22] of all of the R^1−R^4 groups were combined prior to the statistical analysis. For example, in computing the figure for the 3,4-dimethoxy analogue, the MR values of the two methoxy groups plus two hydrogen atoms were added. The following p values were noted when correlations between the physicochemical constants of the aryl substituents and cytotoxicity were obtained. In series **2**, the following relationships were noted (the p values from the linear and semilogarithmic plots, respectively, are in parentheses), namely, π/L1210 (0.042, 0.035), MR/P388 (0.002, 0.010), and MR/Molt 4/C8 (0.071, 0.096). In the case of series **3**, the correlations observed were in the following cases, namely, σ,σ^*/Molt 4/C8 (0.042, 0.044), MR/P388 (0.141, 0.044), and MR/L1210 (0.045, 0.101).

Determination of log P Values of 3a−l. The log P figures were obtained by a literature procedure.[23]

Measurement of Redox Potentials. The E_p values of **1c,i**, **2c,i**, and **3c,i** were determined by a literature procedure.[5] These oxidation potentials were irreversible and are referenced to the silver/silver chloride electrode potential.

Cytotoxicity Evaluations. Compounds were evaluated against murine P388D1 lymphocytic leukemic cells using a literature procedure.[24] A reported methodology was employed

to evaluate the cytotoxic potential of the compounds using murine L1210 lymphoid leukemic cells as well as human Molt 4/C8 and CEM T-lymphocytes.[25]

Determination of the Effect of 1a,l on Macromolecular Biosyntheses. The following method was used for determining the inhibitory effects of **1a,l** on DNA, RNA, and protein biosyntheses in L1210 cells. The tumor cells were seeded in 96 well microtiter plates using $\sim 2 \times 10^5$ cells per well (200 μL) in the presence of different concentrations of **1a,l** and 0.25 μCi of [*methyl*-³H]deoxythymidine, [5-³H]uridine, or [3,4-³H]-leucine. After incubation at 37 °C for 20 h, the trichloroacetic acid−insoluble fractions of the cell cultures were analyzed for radioactivity using a liquid scintillation counter.

Evaluation of Compounds for Anticonvulsant Activity and Neurotoxicity. The enones **1a−l**, **2a−l**, **3a−l**, and **4a−f** were examined for anticonvulsant activity in the MES and scPTZ screens as well as neurotoxicity using a literature procedure.[10] In brief, the compounds were administered intraperitoneally in mice using doses of 30, 100, and 300 mg/kg. After 0.5 and 4 h, any protection against seizures or neurotoxicity was recorded. Using a dose of 300 mg/kg, activity was noted by three compounds in the MES screen, namely, **2f** and **4a** after 0.5 h and **4d** at the end of 4 h. Use of the scPTZ screen revealed that the number of animals protected at 0.5 h after administration were as follows: **2j**, 2/5 at 100 mg/kg, and **3e** and **4a**, 1/5 using 300 mg/kg. Various pathological effects were noted in this screen for the following compounds (dose in mg/kg and time of observation in h in parentheses), namely, continuous seizure activity in the case of **1e** (300, 0.5; 300, 4), **1k** (100,4), and **2e** (300,4), tonic extension with **1k** (30, 0.5) and **2g** (100, 0.5), death following clonic seizure in the case of **2d** (30, 0.5), and myoclonic jerks with **2j** (100, 0.5). The following compounds displayed neurotoxicity (the figures in parentheses indicate the number of animals demonstrating neurological deficit as compared to the total number of mice used, the dose at which neurotoxicity was found, and the time after administration of the compound when toxicity was noted): **1e** (1/8, 100, 0.5); **1f** (1/8, 100, 0.5; 1/4, 300, 0.5); **1g** (2/8, 100, 0.5; 1/4, 100, 4); **1k** (1/8, 100, 0.5; 1/4, 300, 0.5); **1l** (1/4, 30, 0.5; 1/4, 300, 0.5); **2a** (1/4, 30, 0.5; 1/8, 100, 0.5); **2g** (1/4, 300, 0.5); **2l** (1/4, 300, 0.5); **3a** (2/4, 30, 0.5); **3d** (1/8, 100, 0.5; 1/4, 300, 0.5); **3j** (1/4, 300, 0.5; 1/2, 300, 4); **3k** (3/8, 100, 0.5; 1/4, 300, 0.5; 1/4, 100, 4; 1/2, 300, 4); **4e** (1/4, 100, 4; 1/2, 300, 4); and **4f** (1/4, 300, 0.5).

Compounds **1h**,**i**, **2f**,**i**, and **4a** were administered orally to rats using a dose of 30 mg/kg and examined at the end of 0.25, 0.5, 1, 2, and 4 h in the MES and neurotoxicity screens. The following compounds afforded protection in one of four animals (time in h): **1h** (4), **2f** (0.5, 2, 4), and **2i** (1, 4). No protection was noted at any of the times with **1i** and **4a**. None of the compounds demonstrated neurological deficit.

Supporting Information Available: Details of the X-ray crystallographic structures of **1a**,**d**,**h**,**k**,**l**, **2a**,**d−f**,**h**,**j**,**k**, and **3a**,**d**,**e**,**h−j**,**l** including the atomic coordinates and equivalent isotropic displacement parameters, anistropic displacement parameters, hydrogen coordinates and isotropic displacement parameters, and certain bond lengths and bond angles. The d_1-d_4 values determined by X-ray crystallography, comparisons between the d_1-d_{15}, θ_1, and $\psi_1-\psi_5$ figures obtained by X-ray crystallography and molecular modeling for these compounds. This material is available free of charge via the Internet at http://pubs.acs.org.

References

(1) Dimmock, J. R.; Elias, D. W.; Beazely, M. A.; Kandepu, N. M. Bioactivity of chalcones. *Curr. Med. Chem.* **1999**, *6*, 1125−1149.
(2) Dimmock, J. R.; Kandepu, N. M.; Nazarali, A. J.; Kowalchuk, T. P.; Motoganahalli, N.; Quail, J. W.; Mykytiuk, P. A.; Audette, G. F.; Prasad, L.; Perjési, P.; Allen, T. M.; Santos, C. L.; Szdlowski, J.; De Clercq, E.; Balzarini, J. Conformational and quantitative structure−activity relationship study of cytotoxic 2-arylidenebenzocycloalkanones. *J. Med. Chem.* **1999**, *42*, 1358−1366.
(3) Dimmock, J. R.; Kandepu, N. M.; Hetherington, M.; Quail, J. W.; Pugazhenthi, U.; Sudom, A. M.; Chamankhah, M.; Rose, P.; Pass, E.; Allen, T. M.; Halleran, S.; Szydlowski, J.; Mutus, B.; Tannous, M.; Manavathu, E. K.; Myers, T. M.; De Clercq, E.; Balzarini, J. Cytotoxic activities of Mannich bases of chalcones and related compounds. *J. Med. Chem.* **1998**, *41*, 1014−1026.
(4) Suffness, M.; Douros, J. In *Methods in Cancer Research*; DeVita, V. T., Jr., Busch, H., Eds.; Academic Press: New York, 1979; , Vol. XVI, Part A, p 84.
(5) Dimmock, J. R.; Padmanilyam, M. P.; Puthucode, R. N.; Nazarali, A. J.; Motoganahalli, N. L.; Zello, G. A.; Quail, J. W.; Oloo, E. O.; Kraatz, H.-B.; Prisiak, J. S.; Allen, T. M.; Santos, C. L.; Balzarini, J.; De Clercq, E.; Manavathu, E. K. A conformational and structure−activity relationship study of cytotoxic 3,5-bis-(arylidene)-4-piperidones and related *N*-acryloyl analogues. *J. Med. Chem.* **2001**, *44*, 586−593.
(6) Martin, A. R. In *Wilson and Gisvold's Textbook of Organic Medicinal and Pharmaceutical Chemistry*, 10th ed.; Delgado, J. M., Remers, W. A., Eds.; Lippincott-Raven: Philadelphia, 1998; p 212.
(7) Lin, C. M.; Ho, H. H.; Petit, G. R.; Hamel, E. Antimitotic natural products combretastatin A-4 and combretastatin A-2: studies on the mechanism of their inhibition of the binding of colchicine to tubulin. *Biochemistry* **1989**, *28*, 6984−6991.
(8) Pinney, K. G.; Mejia, M. P.; Villalobos, V. M.; Rosenquist, B. E.; Petit, G. R.; Verdier-Pinard, P.; Hamel, E. Synthesis and biological evaluation of aryl azide derivatives of combretastatin A-4 as molecular probes for tubulin. *Bioorg. Med. Chem.* **2000**, *8*, 2417−2425.
(9) Dimmock, J. R.; Kumar, P.; Quail, J. W.; Pugazhenthi, U.; Yang, J.; Chen, M.; Reid, R. S.; Allen, T. M.; Kao, G. Y.; Cole, S. P. C.; Batist, G.; Balzarani, J.; De Clercq, E. Synthesis and cytotoxic evaluation of some styryl ketones and related compounds. *Eur. J. Med. Chem.* **1995**, *30*, 209−217.
(10) Porter, R. J.; Cereghino, J. J.; Gladding, G. D.; Hessie, B. J.; Kupferberg, H. J.; Scoville, B.; White, B. G. Antiepileptic drug development program. *Cleveland Clin. Q.* **1984**, *51*, 293−305.
(11) Dunham, N. W.; Miya, T. S. A note on a simple apparatus for detecting neurological deficit in rats and mice. *J. Am. Pharm. Assoc.* **1957**, *46*, 208−209.
(12) Nelson, A. T.; Houlihan, W. J. The aldol condensation. In *Organic Reactions*; Cope, A. C., Ed.; John Wiley and Sons: New York, 1968; Vol. 16, pp 44−47.
(13) Hassner, A.; Cromwell, N. H. The chemistry of derivatives of benzaltetralone. II. Absorption spectra and stereostructure. *J. Am. Chem. Soc.* **1958**, *80*, 893−900.
(14) Hall, S. R.; King, P. S. D.; Stewart, J. M., Eds. *Xtal 3.4 Users Manual*; University of Western Australia: Perth, 1995.
(15) Gabe, E. J.; LePage, Y.; Charland, J. P.; Lee, F. L.; White, P. S. An interactive program system for structure analyses. *J. Appl. Crystallogr.* **1989**, *22*, 384−387.
(16) Sheldrick, G. M. Program for the refinement of crystal structures; University of Göttingen: Germany, 1977.
(17) Ibers, J. A., Hamilton, W. C., Eds. *International Tables for X-ray Crystallography*; Kynoch Press: Birmingham, U.K., 1974; Vol. IV.
(18) Johnson, C. K. *Ortep II*; Report ORNL-5138; Oak Ridge National Laboratory: Tennessee, 1976.
(19) Mohamadi, F.; Richards, N. G. J.; Gude, W. C.; Liskamp, M. L.; Canfield, C.; Change, G.; Hendrickson, T.; Still, W. C. MacroModel−an integrated software system for modeling organic and bioorganic molecules using molecular mechanics. *J. Comput. Chem.* **1990**, *11*, 440−467.
(20) Perrin, D. D.; Dempsey, B.; Serjeant, E. P. *pKₐ Prediction for Organic Acids and Bases*; Chapman and Hall: London, 1981; pp 109, 112.
(21) Taft, R. W., Jr. In *Steric Effects in Organic Chemistry*; Newman, M. S., Ed.; John Wiley and Sons: New York, 1956; p 591.

(22) Hansch, C.; Leo, A. J. *Substituent Constants for Correlation Analysis in Chemistry and Biology*; John Wiley and Sons: New York, 1979; p 49.

(23) Takács-Novák, K.; Perjési, P.; Vámos, J. Determination of log P for biologically active chalcones and cyclic chalcone analogues by RPTLC. *J. Planar Chromatogr.* **2001**, *14*, 42−46.

(24) Phillips, O. A.; Nelson, L. A.; Knaus, E. E.; Allen, T. M.; Fathi-Afshar, R. Synthesis and cytotoxic activity of pyridylthio, pyridylsulfinyl and pyridosulfonyl methyl acetates. *Drug Des. Delivery* **1989**, *4*, 121−127.

(25) Balzarini, J.; De Clercq, E.; Mertes, M. P.; Shugar, D.; Torrence, P. F. 5-Substituted 2-deoxyuridines: correlation between inhibition of tumor cell growth and inhibition of thymidine kinase and thymidylate synthetase. *Biochem. Pharmacol.* **1982**, *31*, 3673−3682.